Title

Aquaporin-4 Reduces Post-Traumatic Seizure Susceptibility by Promoting Astrocytic Glial Scar Formation in Mice

Journal

Journal of Neurotrauma, 38(8)

ISSN

0897-7151

Authors

Lu, Daniel C
Zador, Zsolt
Yao, Jinghua
et al.

Publication Date

2021-04-15

DOI

10.1089/neu.2011.2114

Peer reviewed

JOURNAL OF NEUROTRAUMA 38:1193–1201 (April 15, 2021)

DOI: 10.1089/neu.2011.2114

Aquaporin-4 Reduces Post-Traumatic Seizure Susceptibility by Promoting Astrocytic Glial Scar Formation in Mice

Daniel C. Lu, Zsolt Zador, Jinghua Yao, Farbod Fazlollahi, and Geoffrey T. Manley

Abstract

Seizures are important neurological complications after traumatic brain injury (TBI) and are reported for up to 50% of patients with TBI. Despite several studies, no drug strategy has been able to alter the biological events leading to epileptogenesis. The glial water channel, aquaporin-4 (AQP4), was shown to facilitate cytotoxic cell swelling in ischemia and glial scar formation after stab wound injury. In this study, we examined post-traumatic seizure susceptibility of AQP4-deficient mice ($AQP4^{-/-}$) after injection of pentylenetetrazole (PTZ) 1 month after controlled cortical impact (CCI) and compared them to wild-type sham injury controls. After PTZ injection, $AQP4^{-/-}$ mice demonstrated dramatically shortened seizure latency (120 ± 40 vs. 300 ± 70 sec; $p < 0.001$) and increased seizure severity (grade 7.5 ± 0.4 vs. 5.8 ± 0.4; $p < 0.001$) compared to their wild-type counterparts. Morphometric analysis demonstrated a significant 2-fold reduction in astrocytosis, with a concomitant increase in microgliosis in injured AQP4-null mice compared to their injured wild-type counterparts (44 ± 2 vs. 24 ± 3 cells per high power field [cells/hpf], respectively; $p < 0.0001$). Minocycline, an inhibitor of microglia, reversed the post-TBI epilepsy phenotype of AQP4-null mice. After minocycline treatment, $AQP4^{-/-}$ mice demonstrated similar latency of seizures evoked by PTZ (723 ± 35 vs. 696 ± 38 sec; $p > 0.05$) and severity of seizures evoked by PTZ (grade 4.0 ± 0.5 vs. 3.81 ± 0.30; $p > 0.05$) compared to wild-type counterparts. Immunohistochemical analysis demonstrated decreased immunostaining of microglia to levels comparable to wild-type (12 ± 2 vs. 11 ± 4 cells/hpf, respectively; $p > 0.05$). Taken together, these results suggest a protective role of AQP4 in post-traumatic seizure susceptibility by promoting astrogliosis, formation of a glial scar, and preventing microgliosis.

Keywords: aquaporin; astrocyte; glial scar; seizure epilepsy

Introduction

Post-traumatic seizures (PTSs) are a well-known complication of traumatic brain injury (TBI), and post-traumatic epilepsy (PTE) accounts for 20% of all symptomatic epilepsy in the general population.[1–3] PTSs are classified as immediate seizures (<24 h after injury), early seizures (<1 week after injury), and late seizures (>8 days after injury).[4] Current treatment of early PTS has been the use of antiepileptic medication; however, the ability to prevent the development of late seizures after TBI with early antiepileptic medication has not been demonstrated.[5,6] Additionally, the side effects of seizure medications often preclude its prolonged use. Therefore, it is important to investigate new approaches in the prevention of PTE.

Aquaporins are a family of membrane proteins that function as ''water channels'' in many cell types and tissues in which fluid transport is crucial.[7] There is evidence that water movement in the brain involves aquaporin channels.[8,9] Aquaporin-4 (AQP4) is expressed ubiquitously by glial cells, especially at specialized membrane domains including astroglial endfeet in contact with blood vessels and astrocyte membranes that ensheath glutamatergic synapses.[10,11] Activity-induced radial water fluxes in neocortex have been demonstrated that could be attributable to water movement through aquaporin channels in response to physiological activity.[12,13] Additionally, AQP4 promotes astrocyte migration, and AQP4-null animals have demonstrated delayed astrocyte movement.[14,15]

Astrocytes in the healthy brain mediate glutamate reuptake, regulate the ionic environment and interstitial volume, and serve as a component of the neurovascular unit that controls blood–brain barrier permeability.[16] Although reactive astrocytes in the epileptic focus are known to undergo extensive morphological and physiological changes that modify these three overarching functions, the implications for epilepsy are just emerging. In models of TBI, conditional ablation of proliferating astrocytes increases neuronal injury and increases infiltration of damaged region by microglia.[17,18] These data strongly point to a protective function of proliferating astrocytes.

Department of Neurological Surgery, University of California, San Francisco, San Francisco, California, USA.

However, there is also evidence that suggests that reactive astrocytes might contribute to the hyperexcitable condition. During the epileptic state, there is a redistribution of AQP4 away from the perivascular membranes toward neuropil, which should create a situation allowing rapid astrocytic swelling in the neuropil with consequent shrinkage in extracellular space and enhanced ephaptic interactions among tightly packed neurons.[19] Additionally, neuroinflammatory signaling pathways engaged in reactive glia in epileptic foci may allow astrocytic glutamate signaling to become prominent enough to contribute to the hyperexcitable state. Together, these factors argue for a hyperexcitable role in reactive astrocytes.

In this study, we utilized AQP4-null mice, taking advantage of the known function of AQP4 in astrocyte migration and K^+ buffering, to elucidate its role in mediating susceptibility to seizures. We demonstrate that susceptibility to seizures is significantly higher in mice lacking AQP4 in a pentylenetetrazole (PTZ)-induced seizure model.[20] We also demonstrate that seizure phenotype is related to decreased astroglia migration and, consequently, increased microglia formation. Last, we show that inhibition of microglia by minocycline treatment abolishes this seizure phenotype in AQP4-null mice.

Methods

AQP4$^{-/-}$ mice

All animal procedures were approved by the University of California, San Francisco committee on Animal Research. AQP4$^{-/-}$ mice were generated as previously described by Ma and colleagues.[21] These mice lacked detectable AQP4 protein and phenotypically have normal growth, development, survival, and neuromuscular function. A total of 40 wild-type mice and 40 AQP4-deficient mice were subjected to initial seizure testing, with 20 wild-type and 20 AQP4-null in the sham group and 20 wild-type and 20 AQP4-null in the CCI group. In the minocycline seizure experiments, a total of 24 wild-type and 24 AQP4-deficient mice were used, with 12 wild-type and 12 AQP4-null mice in the saline-treated group and 12 wild-type and 12 AQP4-null mice in the minocycline-treated group.

Controlled cortical impact

Mice (12 weeks of age) were anesthetized with 4% isoflurane (Anaquest, Memphis, TN) in 70% N2O and 30% O2 using a Fluotec 3 vaporizer (Colonial Medical, Amherst, NH) and positioned in a stereotactic frame. Anesthesia was maintained using 2–3% isoflurane. A 5-mm craniotomy was made using a portable drill and trephine over the left parietotemporal cortex (the center of the coordinates of craniotomy relative to bregma: 1.5 mm posterior, 2.5 mm lateral), and the bone flap was removed. Mice were then subjected to CCI using a pneumatic cylinder with a 3-mm flat-tip impounder (E-CCI Model 6.3; Custom Design and Fabrication, New York, NY), velocity 6 m/sec, set to depth of 1.2 mm, and 100-ms impact duration. The bone flap was then replaced and secured with tissue sealant (Abbott Laboratories, North Chicago, IL). The scalp was sutured closed and mice returned to their cages to recover. Body temperature was monitored by a rectal probe and maintained with a heating pad throughout the procedure to a temperature of 38.0°C. There were two mortalities associated with CCI in the initial seizure cohort: one in the wild-type and another in the AQP4-null mice. Another mortality was present in a minocycline-treated wild-type mouse after CCI.

Assessment of seizure susceptibility

One month after initial CCI, seizures were induced by PTZ (Sigma-Aldrich, St. Louis, MO). PTZ was dissolved in phosphate-buffered saline (PBS) and delivered by intraperitoneal injection. PTZ was used at a concentration of 5 mg/mL and a dose of 40 mg/kg. For mice given PTZ, each mouse was placed in a cage and observed for 20 min after administration, with video recording. An investigator blinded to genotype analyzed the videotapes to quantify the time course, latency,[22] and severity of seizures according to published scales.[20] Seizure severity scores were: 0 = normal behavior; 1 = immobility; 2 = generalized spasm, tremble, or twitch; 3 = tail extension; 4 = forelimb clonus; 5 = generalized clonic activity; 6 = bouncing or running seizures; 7 = full tonic extension; and 8 = death. A pilot study showed that animals do not show increased seizure activity beyond 20 min past PTZ induction. It was also shown that seizures do not evolve further after this 20-min period, and length of seizures was unrelated to experimental group. Therefore seizures were scored as the greatest seizure activity within the 20-min observation period.

Immunostaining

Immediately after assessment of seizure susceptibility, mice were anesthetized by an intraperitoneal injection of Avertin (125 mg/kg) and perfused transcardially with 4% paraformaldehyde in PBS. Mice were decapitated, and then the brain was dissected and post-fixed for 24 h in paraformaldehyde at 20°C. Tissues were dehydrated with increasing concentrations of ethanol, treated with clearing agent, and embedded in paraffin. Some sections were deparaffinized and stained with cresyl violet (Nissl stain), using standard procedures. For immunofluorescence, epitope exposure was enhanced by incubation in citrate buffer (10 mM of sodium citrate, 0.05% Tween 20, pH 6.0; 30 min, 95°C–100°C). Sections were blocked with bovine serum albumin (3%), incubated with polyclonal anti-AQP4 antibody (1:200), monoclonal CD11b antibody (1:200), or polyclonal anti–glial fibrillary acidic protein (GFAP; 1:200) for 4 h at room temperature (Millipore, Billerica, MA), followed by Texas Red donkey/antirabbit (1:200) or biotinylated secondary antibody (1:200), and avidin horseradish peroxidase for GFAP and CD11b (Vector Laboratories, Burlingame, CA). Immunolabeling was visualized brown using diaminobenzidine.

Lesion volume was assessed by digital images (8-bit jpeg format) taken of five consecutive Nissl-stained coronal sections through the injury site (200-μm separation). We used ImageJ (v. 1.33u; NIH, Bethesda, MD) to arbitrarily set pixels with intensities 175–255 as white, and the remaining pixels (intensities 0–174) blue, and calculated the percentage of white pixels in each image.

A cell-counting procedure was performed with a 60× objective to quantify positive cells to each antibody tested. Sections with the highest positive cell density were taken, and an average of five different coronal sections was used for each mouse (7 mice for each treatment group, 28 mice total). Data are presented as mean ± standard error. The experimenter performing the cell count was blinded to the genotype and treatment.

Scanning confocal laser microscopy

Immunostained sections were mounted in Vectashield Fluorescent Mounting Media (Vector Laboratories) and imaged using a Nikon Eclipse FN1 Upright Microscope or Nikon Eclipse C1si Confocal Microscope with a 20×/0.75 Air-Plan Apo (DIC N2; Nikon Instruments Inc., Melville, NY) objective at a resolution of 512×512 pixels to 1024×1024 pixels. Nikon C1 acquisition software and NIS Elements software for three-dimensional (3D) reconstructions were used and sampled from a thickness of 50 μm with a Z step of 1 μm. Sections from each cohort ($n = 6$ in each) and condition were analyzed, and representative images are shown.

Minocycline treatment

Minocycline HCl (Sigma-Aldrich) was administered intraperitoneally 12 h before TBI at a dose of 45 mg/kg body weight. This dose was selected based on previous studies.[23,24] Beginning 30 min after trauma, animals received minocycline injections every 12 h, at a dose of 90 mg/kg for the first 24 h after trauma and then 45 mg/kg thereafter until mice were euthanized. Control animals received equivalent saline volume.

Statistical analysis

A value of $p < 0.05$ was considered significant. Error bars represent standard error of the mean. Genotype and treatment (CCI or minocycline) differences were analyzed by one-way analysis of variance, followed by Tukey-Kramer's test of *post hoc* comparisons.

Results

Increased seizure severity and decreased seizure latency in post-traumatic aquaporin-4-null mice

Seizure susceptibility after CCI was assessed by the well-established γ-aminobutyric acid type A (GABAA) receptor-antagonist PTZ-induced seizure assay. As expected, animals showed significantly increased seizure severity after CCI for both genotypes (Fig. 1A). Interestingly, brain-injured AQP4-null mice demonstrated a significantly increased seizure severity compared to wild-type mice (Fig. 1C).

Seizure latency to stage 5 (generalized clonic activity) was measured in the animals above (Fig. 1B). Sham AQP4-null mice at baseline were resistant to PTZ-induced seizures compared to their wild-type counterparts. Additionally, CCI increased the sensitivity of mice to PTZ-induced seizures by decreasing eizure latency. Interestingly, AQP4-null mice had decreased latency after CCI as compared to wild type. These results establish that AQP4-null mice have a significantly worse seizure response after TBI. To investigate the cellular mechanisms responsible for these seizure findings, we conducted immunohistochemical studies to assess injury characteristics and specific markers pertinent to the known functions of AQP4 in glial scar formation.

Similar injury volume in aquaporin-4-null and wild-type mice after controlled cortical impact

To determine whether there was a difference in injury volume between wild-type versus AQP4-null mice, Nissl staining of coronal brain sections was performed (Fig. 2A). Grossly, there were no observed differences in the extent of injury between genotypes. The cortex beneath the impact site was obliterated with some perturbation to the underlying hippocampus. Quantifying the volume of injury demonstrated no genotype difference (Fig. 2B). Given that there was no difference in injury volume between the genotypes, we further investigate the mechanism of seizure phenotype by other markers.

Increased aquaporin-4 immunoreactivity after controlled cortical impact

To confirm the knockout genotype and expression pattern of AQP4 after CCI, we performed immunolocalization for AQP4 after CCI in wild-type and AQP4-null mice (Fig. 3A). As expected, there was no immunoreactivity in AQP4-null mice before or after injury,

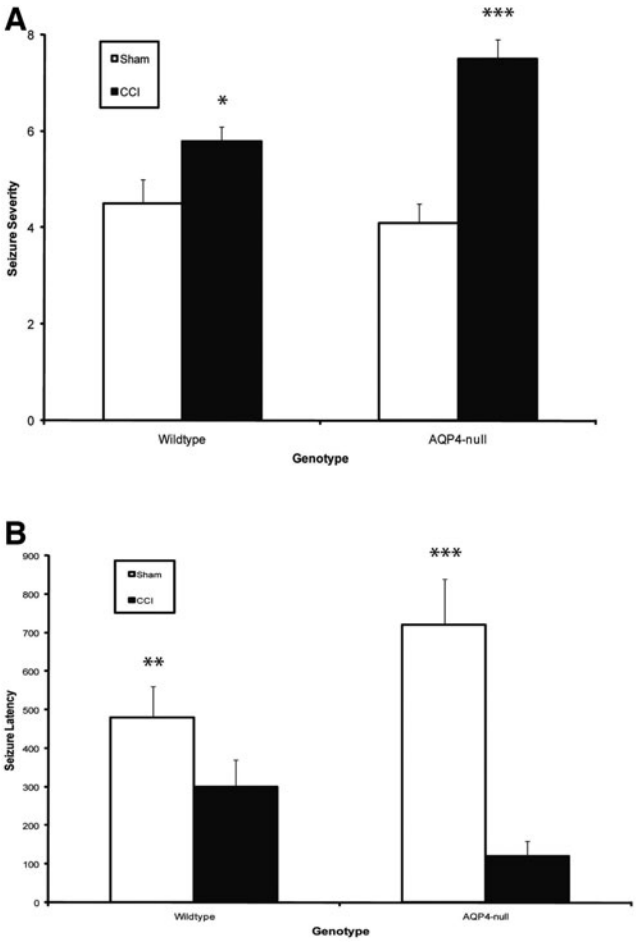

FIG. 1. AQP4-null mice exhibited worse seizure profile after CCI. (**A**) Seizure severity in response to PTZ in wild-type and AQP4-null mice were measured before and after CCI. CCI increased seizure severity in each genotype (*$p < 0.05$ in wild-type and ***$p < 0.001$ in AQP4-null mice). Seizure was more severe in AQP4-null mice (grade 7.5) compared to wild-type mice (grade 4.2; ***$p < 0.001$). (**B**) Seizure latency was measured in the same cohort. Seizure latency was shortened after CCI in both wild-type and AQP4-null mice (**$p < 0.01$ in wild-type and ***$p < 0.001$ in AQP4-null mice). Seizure latency was increased in AQP4-null mice (720 ± 120 sec) compared to wild-type (480 ± 80 sec) before injury. In contrast, after injury, seizure latency was shortened in AQP4-null mice (120 ± 40 sec) compared to wild-type mice (300 ± 70 sec; $p < 0.0001$). *$p < 0.05$; **$p < 0.001$; ***$p < 0.0001$; error bars, $\pm$ standard error of the mean. AQP4, aquaporin-4; CCI, controlled cortical impact.

but a baseline diffuse immunostaining was present in wild-type mice. Interestingly, after injury, AQP4 immunoreactivity increases within the injury region, suggesting migration of AQP4 positive-cells within the region or upregulation of AQP4 within the reactive glial cells. This was assessed by quantitative cell count with high-power microscopic magnification (Fig. 3B).

Decreased astrogliosis in aquaporin-4-null mice after controlled cortical impact

AQP4 has been implicated in glial migration, and astrogliosis is a common phenomenon after CCI. We therefore evaluated whether

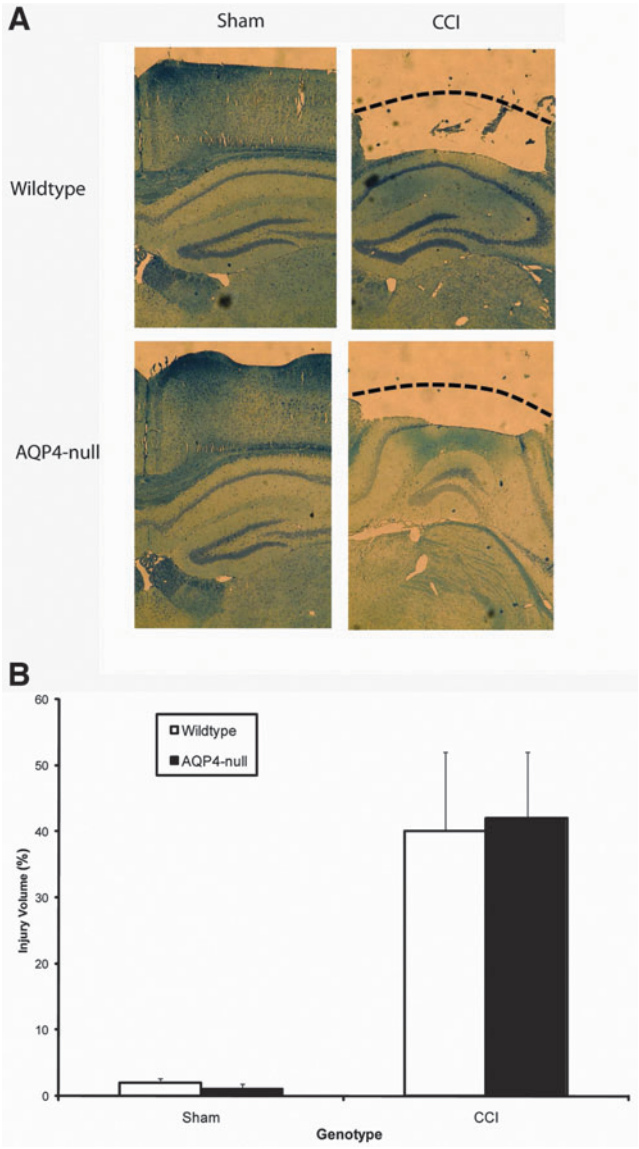

FIG. 2. Similar injury volume in wild-type and AQP4-null mice after CCI. (**A**) Representative brightfield images of Nissl-stained coronal images of wild-type and AQP4-null mice before and after injury are shown (injured region under dotted line). (**B**) Injury volume was quantified and assessed. Genotype did not contribute to differences in injury volume ($p > 0.05$); however, there was a significant CCI effect ($p < 0.001$). In both genotypes, CCI induced an injury volume of $\sim 40\%$. $^{*}p < 0.05$; $^{**}p < 0.001$; $^{***}p < 0.0001$; error bars, ± standard error of the mean. AQP4, aquaporin-4; CCI, cpnmtrolled cortical impact.

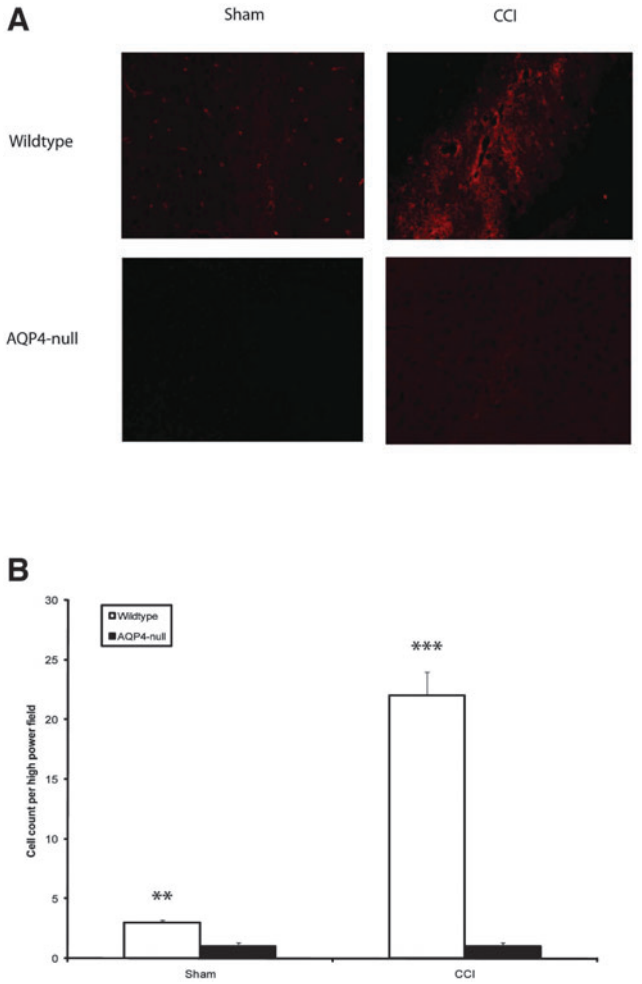

FIG. 3. Increased AQP4 immunoreactivity in injury zone after CCI. (**A**) Representative immunofluorescence images, taken from injury penumbra (immediately adjacent to injury area), showing AQP4 positive cells (red) in wild-type mice. Injury induced clustering and migration of AQP4-positive astrocytes to the injury area. Background immunoreactivity was observed in AQP4-null mice. (**B**) Quantification of AQP4-positive cells surrounding the injury area. Injury strongly increased the number of AQP4-reactive cells in wild-type animals (3.0 ± 0.3 cells/hpf before injury to 24 ± 3 cells/hpf after injury; $p < 0.0001$). This was not observed in AQP4-null mice. As expected, there was a significant difference in AQP4 staining in wild-type compared to AQP4-null mice ($^{**}p < 0.001$ in sham and $^{***}p < 0.0001$ in CCI comparisons). $^{*}p < 0.05$; $^{**}p < 0.001$; $^{***}p < 0.0001$; error bars, ± standard error of the mean. AQP4, aquaporin-4; CCI, controlled cortical impact.

there is a difference in astrocytosis surrounding the impact zone between wild-type and AQP4-null mice after CCI. Indeed, we discovered a significant difference in astrocyte density between wild-type and AQP4-null mice (Fig. 4B). When compared, there were visibly fewer activated astrocytes in AQP4-null versus wild-type mice. After quantification, there was a 2-fold increase in the number of reactive astrocytes after CCI in wild-type mice compared to AQP4-null mice. As control, there were no baseline differences in reactive astrocyte count between sham wild-type and AQP4-null mice. These results confirm the decrease in the number of reactive astrocytes in AQP4-deleted animals after CCI. To evaluate the impact of reactive astrocytes on microglia, we stained these same sections for CD11b, a microglial marker.

Increased microgliosis in aquaporin-4-null mice after controlled cortical impact

Microglia are the immunoeffector cells of the brain. To assess microglia density, we utilized CD11b antibody. We discovered

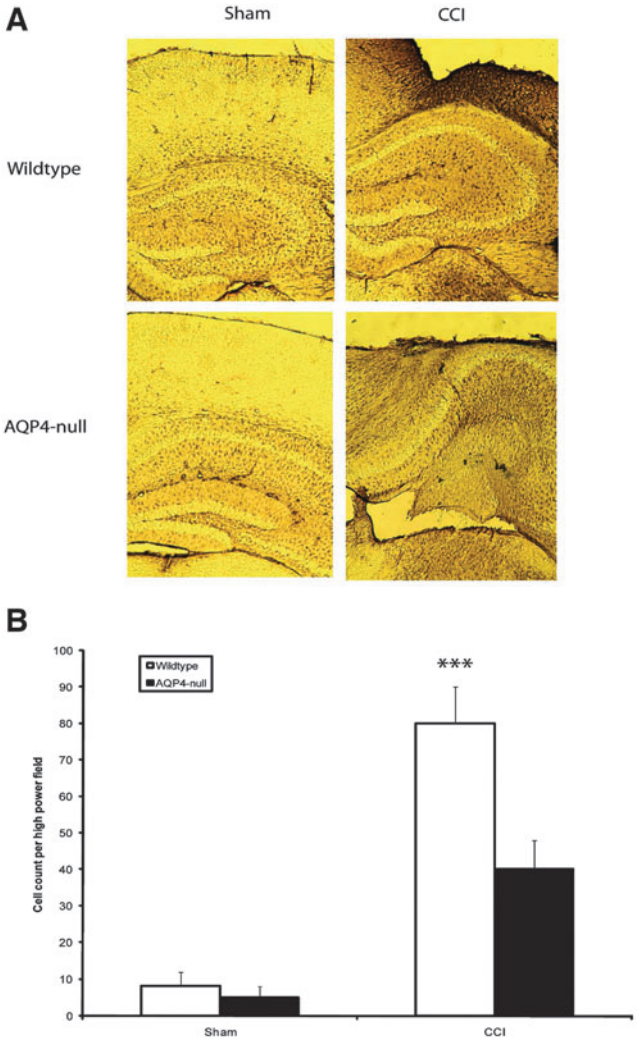

FIG. 4. Reactive astrocytes in injury penumbra after CCI. (**A**) Representative brightfield images showing a dramatic increase in GFAP reactivity in the injury penumbra after CCI in wild-type mice. This increase was observed in cortical regions above the hippocampus. (**B**) Quantification of GFAP-positive cells demonstrated a 2-fold difference in GFAP-positive cells after injury in wild-type versus AQP4-null mice (82 ± 10 vs. 40 ± 8 cells/hpf, respectively; $^{***}p < 0.0001$). This difference between the genotype was not observed in uninjured control mice ($p > 0.05$). $^{*}p < 0.05$; $^{**}p < 0.001$; $^{***}p < 0.0001$; error bars, ± standard error of the mean. AQP4, aquaporin-4; CCI, controlled cortical impact; GFAP, glial fibrillary acidic protein.

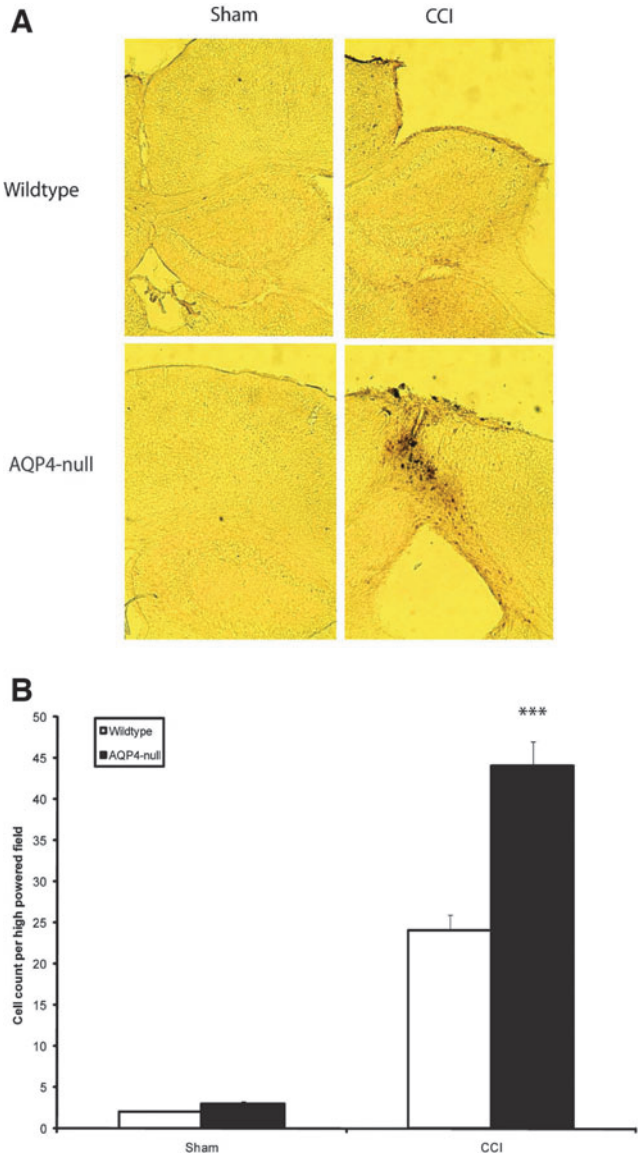

FIG. 5. Microgliosis in injury penumbra after CCI. (**A**) Representative brightfield images showing an increase in CD11b reactivity in the injury penumbra after CCI in AQP4-null mice. (**B**) Quantification of CD11b-positive cells demonstrated a significant difference in CD11b-positive cells after injury in wild-type versus AQP4-null mice (24 ± 3 vs. 44 ± 2 cells/hpf, respectively; $^{***}p < 0.0001$). This difference in genotype was not observed in uninjured control mice (2.0 ± 0.2 vs. 3.0 ± 0.4 cells/hpf, respectively; $p > 0.05$). $^{*}p < 0.05$; $^{**}p < 0.001$; $^{***}p < 0.0001$; error bars, ± standard error of the mean. AQP4, aquaporin-4; CCI, controlled cortical impact.

that indeed this difference in astrocytosis translates into differences in microglia scar density. Qualitatively, we observed an obvious difference in the sections (Fig. 5A), and found that wild-type mice had less CD11b reactivity compared to AQP4-null mice after injury. Quantitatively, we discovered a significantly increased microgliosis in AQP4-null mice compared to wild-type mice after CCI (Fig. 5B). There was minimal CD11b activation in non-injured controls. These results indicate that AQP4 deletion results in increased microglia accumulation in areas of injury.

Decreased astrocytic glial scar in aquaporin-4-null mice after controlled cortical impact

To look closely at the 3D morphology of the glial scar, we utilized scanning confocal laser microscopy on brain sections costained with GFAP and AQP4 (Fig. 6). Morphologically, in the wild-type mice, there is a robust astrocytic glial scar surrounding the injured cavity (white). This scar can be visualized as a barrier to the injured tissue; whereas in the AQP4-null mice, this scar formation was weak. To confirm AQP4 expression in

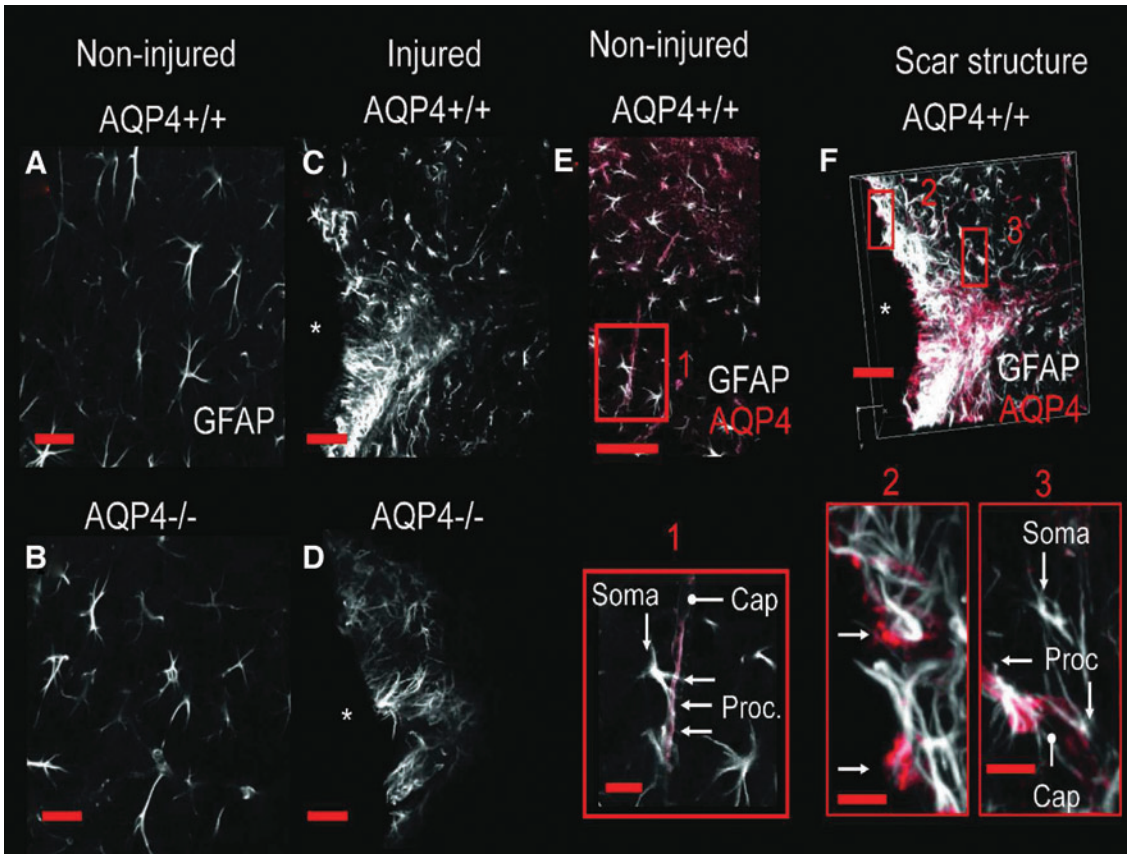

FIG. 6. Astrocytic scar morphology after CCI. Expression pattern of GFAP and AQP4 after cortical contusion. Immunolabeling of GFAP (white) in the cerebral cortex of uninjured $AQP4^{+/+}$ (**A**) and $AQP4^{-/-}$ mice (**B**) demonstrated similar astrocyte morphology. Expression of GFAP in the glial scar lining the injury cavity in $AQP4^{+/+}$ (**C**) and $AQP4^{-/-}$ (**D**) mice. After injury, there was robust GFAP immunoreactivity in (C) wild-type mice compared to (D) weaker GFAP immunostaining of AQP4-deficient mice. (**E**) Expression of AQP4 (red) in GFAP-positive (white) astrocyte endfeet in non-injured $AQP4^{+/+}$ mice (inset 1). Note the predominant pericapillary AQP4 expression pattern of astrocytic foot processes. Expression pattern AQP4 in GFAP-positive astrocytes in the glial scar after injury (**F**) adjacent to the injury cavity (inset 2): note the AQP4 positive astrocyte cell bodies (arrows). In regions distal from the injury core (inset 3), note the perivascular pattern of AQP4 staining. Scale bars: A,B: 40 μm; C,D,E: 120 μm; F, inset 1, 2, and 3: 10 μm. Asterisk (''*'') denotes injury core. $*p<0.05$; $**p<0.001$; $***p<0.0001$; error bars, ± standard error of the mean. AQP4, aquaporin-4; CCI, controlled cortical impact; GFAP, glial fibrillary acidic protein.

the wild-type mice and lack of expression in AQP4-null mice, sections were costained with AQP4 antibody (red). As expected, AQP4-null mice did not have appreciable staining with AQP4 antibody. There appears to be a differential expression pattern of AQP4 in regions surrounding the injury cavity (somal pattern, A) as compared to regions near normal brain (pericapillary pattern, B).

Minocycline treatment reverses seizure phenotype in aquaporin-4-null mice

To assess the effect of minocycline on seizure severity, AQP4-null and wild-type mice were subjected to PTZ-induced seizure assay. In the saline control cohort, as expected, AQP4-null mice demonstrated more severe seizures as compared to wild-type mice after injury ($p<0.0005$); however, after minocycline treatment, seizure severity in AQP4-null mice decreased to a similar level as compared to its wild-type counterpart after injury (Fig. 7A). Further, minocycline had a significant inhibitory effect on seizure severity in wild-type mice as well. Seizure latency correspondingly increased with the treatment of minocycline after injury as compared to saline control in both AQP4-null and wild-type mice (Fig. 7B).

Minocycline treatment diminishes microgliosis without affecting injury volume, aquaporin-4 immunoreactivity, or astrocytosis

In looking for causes of the above seizure phenomenon, we subjected brain slices of the injured minocycline- and saline-treated mice to Nissl staining, in addition to AQP4, GFAP, and CD11b antibodies to assay injury volume, AQP4 immunoreactivity, astrocytosis, and microgliosis, respectively (Fig. 8). Minocycline treatment did not have an appreciable effect on injury volume (Fig. 8A), AQP4 immunoreactivity (Fig. 8B), nor GFAP immunoreactivity (Fig. 8C) as compared to saline control. In contrast, minocycline-treated animals had substantially decreased CD11b immunoreactivity as compared to saline-treated controls, such that there was no statistical difference

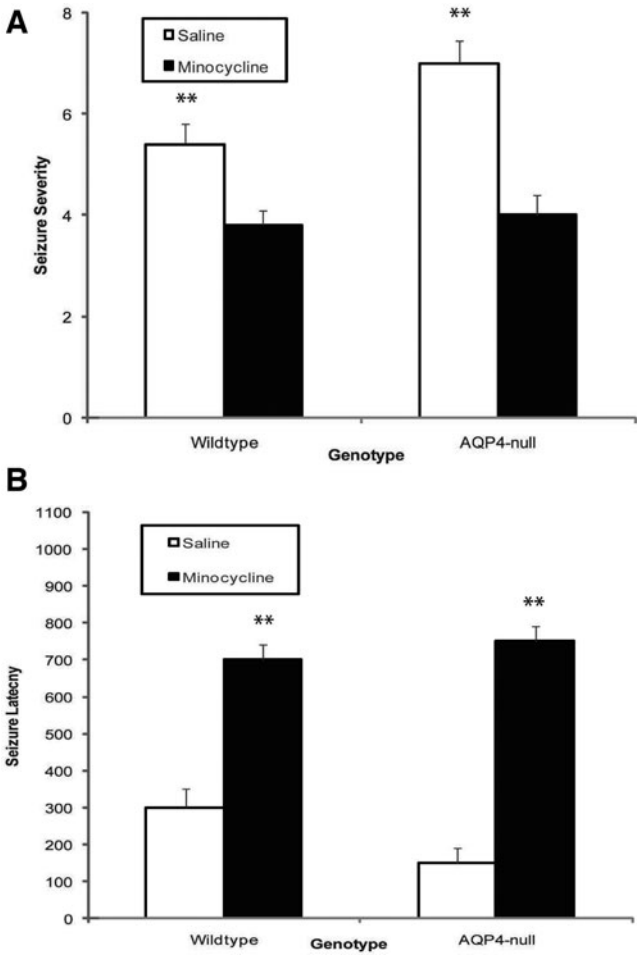

FIG. 7. Minocycline treatment reverses seizure profile of AQP4-null mice after CCI. (**A**) Seizure severity in response to PTZ in wild-type and AQP4-null mice was measured in saline- and minocycline-treated animals subjected to CCI. Minocycline reduced the seizure severity in wild-type and AQP4-null cohorts compared to saline control ($^{**}p < 0.001$). There was no genotype difference in seizure severity of minocycline-treated animals ($p > 0.05$). (**B**) Seizure latency was increased after minocycline treatment in AQP4-null and wild-type mice (analysis of variance treatment effect, $^{**}p < 0.001$). There was no genotype difference in seizure latency of minocycline-treated animals ($p > 0.05$). $^{*}P < 0.05$; $^{**}P < 0.001$; $^{***}P < 0.0001$; error bars, ± standard error of the mean. AQP4, aquaporin-4; CCI, cpnmtrolled cortical impact; PTZ, pentylenetetrazole.

between the two genotypes (Fig. 8D). This inhibitory effect of minocycline on microgliosis was present in both wild-type and AQP4-null mice.

Discussion

The principal finding of this study is an increase in seizure susceptibility in AQP4-deficient mice after CCI injury, with reduced astrocytes and increased microglia within the injury region. Inhibition of microgliosis by minocycline reversed the seizure phenotype in these AQP4-deficient mice. These observations imply that glial scar formation is protective against post-traumatic seizures by a microglia-dependent mechanism.

Immunohistochemical studies demonstrated similar injury volume, decreased reactive astrocytes, and increased microglia in AQP4 knockout animals after CCI. Further, strongly AQP4-positive astrocytes were present within the glial scar of wild-type animals. These findings suggest that reactive astrocytes play a therapeutic role in the repair of the injured area by displacing microglial cells. Several lines of evidence show that the deletion of AQP4 results in reduction of the astrocytic component of the glial scar in various pathologies.[14,15] It has been proposed that, as a water channel, AQP4 polarizes at the leading edge of the migrating astrocytes and thus enhances cellular water uptake and cell volume changes to facilitate cell movement.[25] Consistent with this hypothesis, AQP4 expression was shown to enhance the reactive astrocytes of the glial scar. Microglia are leukocytes of the central nervous system (CNS) and perform phagocytic functions. In higher vertebrates, leukocytes gain little entry into normal CNS parenchyma; therefore, CNS inflammatory response to injury differs from that of other tissues.[26,27] After injury, blood-borne monocytes and lymphocytes gain delayed and limited access to CNS parenchyma.[27–29] However, in the absence of astrocytes, leukocytes gain increased and prolonged entry into CNS parenchyma.[17] Previously, the peripheral inflammation model of microglia activation has been linked to CNS excitability. Microglia inhibition by minocycline prevented the increase in seizure susceptibility.[30] Recently, minocycline has been demonstrated to be a selective inhibitor of microglia activation in various disease models from cerebral ischemia to intracerebral hemorrhage.[31–34]

In our study, the prolonged and increased presence of microglia may present a pathogenic mechanism for inflammatory disturbance that could alter seizure susceptibility. Indeed, such a mechanism is supported by our observation that microglia inhibition with minocycline reverses the seizure phenotype of AQP4-null mice.

Reactive astrocytes are known to demonstrate enhanced inwardly rectified K^+ currents,[35] which suggest their role of enhancing K^+ uptake during neuroexcitation.

The differential expression pattern of AQP4 within the injury penumbra as we observed may impact K^+ buffering given that AQP4 is associated and colocalizes with the inwardly rectifying K^+ channel, Kir4.1,[36] and within this association, AQP4 is proposed to act as an ion-water trafficking protein to facilitate K^+ clearance. Absence of such a mechanism may lead to lower seizure threshold[37–39] in AQP4-null mice and contribute to the AQP4-null seizure phenotype after CCI. However, in our study, given that inhibition of microglia activation reverses much of the seizure phenotype in AQP4-null mice, the contribution of K^+ uptake in this injury model may be modest.

Our present study is the first to demonstrate *in vivo* the beneficial role of glial scar formation in post-traumatic seizures using a transgenic mouse model. Clinically, glial scarring has been determined as a contributor to the pathogenesis of epilepsy, and treatment consists of surgical resection, as in the case of mesial temporal sclerosis, after failing medical treatment (both in traumatic and non-traumatic cases). However, failure rates are high, and our current study may provide a mechanistic understanding of the failure. During the repair phase of the surgical site, the proepileptic effects of microglia may predominate.

Further, our findings may be relevant not only in the TBI setting, but also to surgical treatment of the CNS disorders where surgical trauma is introduced and post-operative antiepileptic medications are used. This study suggests that inhibition of microglia or reinforcement of AQP4 function in reactive astrocytes may serve as a potential therapeutic target to mitigate epileptogenesis after brain injury.

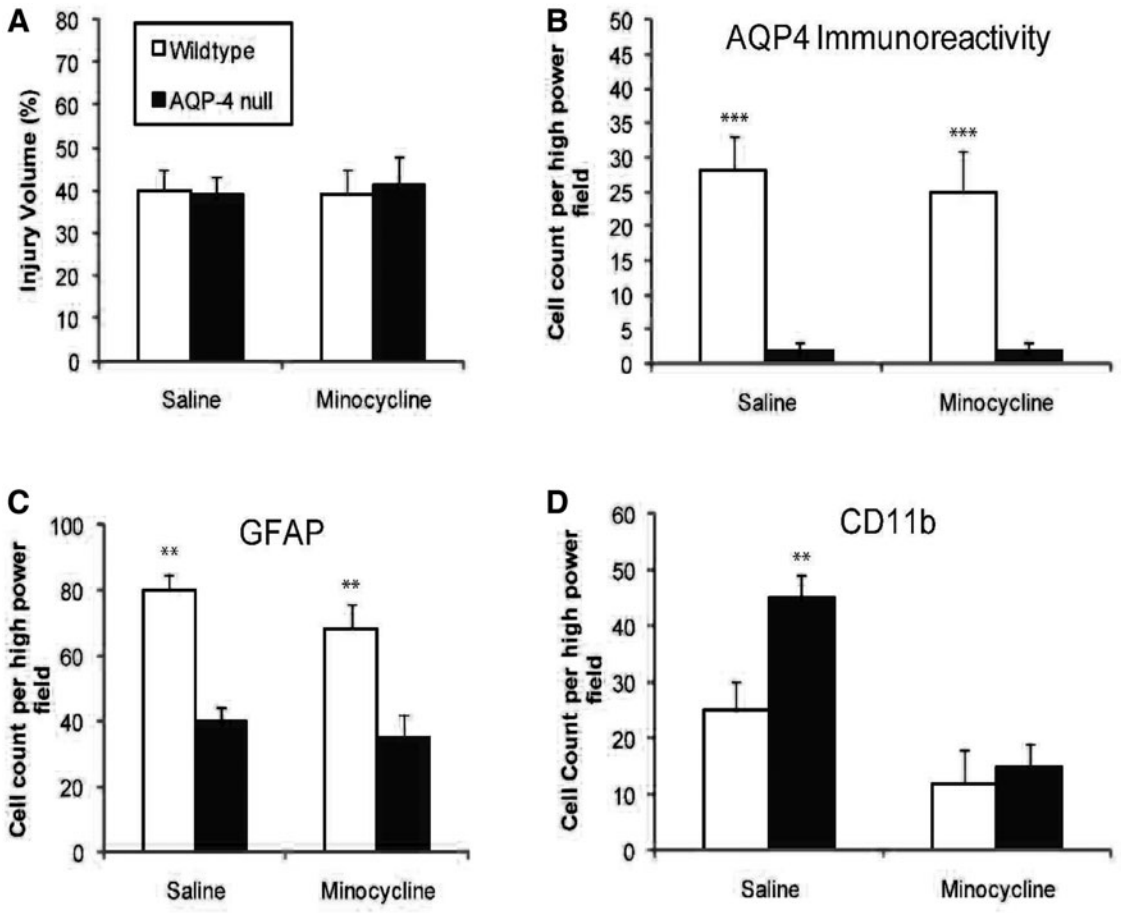

FIG. 8. Minocycline treatment inhibits microgliosis. (**A**) Injury volume was quantified and assessed by Nissel staining. Minocycline did not have an effect on injury volume ($p > 0.05$). In both genotypes, CCI induced an injury volume of $\sim 40\%$. (**B**) Quantification of AQP4-positive cells surrounding injury area. There was no difference in AQP4 immunoreactivity in the wild-type cohort with saline or minocycline treatment ($p > 0.05$). As expected, there was background AQP4 staining in AQP4-null mice with robust staining in the wild-type cohort ($^{***}p < 0.001$). (**C**) Quantification of GFAP-positive cells demonstrated an ~ 2-fold difference in GFAP-positive cells in wild-type versus AQP4-null injured mice in both saline- and minocycline-treated animals ($^{**}p < 0.001$). There was no observed GFAP cell count difference between the saline- and minocycline-treated cohorts ($p > 0.05$). (**D**) Quantification of CD11b-positive cells demonstrated a significant increase in CD11b-positive cells in saline-treated wild-type vs. AQP4-null mice (25 ± 6 vs. 45 ± 4 cells/hpf, respectively; $^{**}p < 0.001$). This difference in genotype was not observed in minocycline-treated mice (11 ± 4 vs. 12 ± 2 cells/hpf, respectively; $p > 0.05$) given that minocycline-treatment decreased CD11b-positive cells regardless of genotype. $^{*}p < 0.05$; $^{**}p < 0.001$; $^{***}p < 0.0001$; error bars, $\pm$ standard error of the mean. AQP4, aquaporin-4; CCI, controlled cortical impact; GFAP, glial fibrillary acidic protein.

Funding Information

This work was supported by a grant from the National Institutes of Health (R01 NS050173-01A1).

Author Disclosure Statement

No competing financial interests exist.

References

1. Annegers, J.F., and Coan, S.P. (2000). The risks of epilepsy after traumatic brain injury. Seizure 9, 453–457.
2. Jennett, B., Teather, D., and Bennie, S. (1973). Epilepsy after head injury. Residual risk after varying fit-free intervals since injury. Lancet 2, 652–653.
3. Semah, F., Picot, M.C., Adam, C., Broglin, D., Arzimanoglou, A., Bazin, B., Cavalcanti, D., and Baulac, M. (1998). Is the underlying cause of epilepsy a major prognostic factor for recurrence? Neurology 51, 1256–1262.
4. Iudice, A., and Murri, L. (2000). Pharmacological prophylaxis of post-traumatic epilepsy. Drugs 59, 1091–1099.
5. Teasell, R., Bayona, N., Lippert, C., Villamere, J., and Hellings, C. (2007). Post-traumatic seizure disorder following acquired brain injury. Brain Inj. 21, 201–214.
6. Temkin, N.R., Dikmen, S.S., Wilensky, A.J., Keihm, J., Chabal, S., and Winn, H.R. (1990). A randomized, double-blind study of phenytoin for the prevention of post-traumatic seizures. N. Engl. J. Med. 323, 497–502.
7. Verkman, A.S. (2005). Novel roles of aquaporins revealed by phenotype analysis of knockout mice. Rev. Physiol. Biochem. Pharmacol. 155, 3155.
8. Amiry-Moghaddam, M., Williamson, A., Palomba, M., Eid, T., de Lanerolle, N.C., Nagelhus, E.A., Adams, M.E., Froehner, S.C., Agre, P., and Ottersen, O.P. (2003). Delayed K^+ clearance associated with aquaporin-4 mislocalization: phenotypic defects in brains of alpha-syntrophin-null mice. Proc. Natl. Acad. Sci. U. S. A. 100, 13615–13620.
9. Manley, G.T., Binder, D.K., Papadopoulos, M.C., and Verkman, A.S. (2004). New insights into water transport and edema in the central

nervous system from phenotype analysis of aquaporin-4 null mice. Neuroscience 129, 983–991.
10. Nagelhus, E.A., Mathiisen, T.M., and Ottersen, O.P. (2004). Aquaporin-4 in the central nervous system: cellular and subcellular distribution and coexpression with KIR4.1. Neuroscience 129, 905–913.
11. Nielsen, S., Nagelhus, E.A., Amiry-Moghaddam, M., Bourque, C., Agre, P., and Ottersen, O.P. (1997). Specialized membrane domains for water transport in glial cells: high-resolution immunogold cytochemistry of aquaporin-4 in rat brain. J Neurosci 17, 171–180.
12. Holthoff, K., and Witte, O.W. (2000). Directed spatial potassium redistribution in rat neocortex. Glia 29, 288–292.
13. Niermann, H., Amiry-Moghaddam, M., Holthoff, K., Witte, O.W., and Ottersen, O.P. (2001). A novel role of vasopressin in the brain: modulation of activity-dependent water flux in the neocortex. J. Neurosci. 21, 3045–3051.
14. Auguste, K.I., Jin, S., Uchida, K., Yan, D., Manley, G.T., Papadopoulos, M.C., and Verkman, A.S. (2007). Greatly impaired migration of implanted aquaporin-4-deficient astroglial cells in mouse brain toward a site of injury. FASEB J. 21, 108–116.
15. Saadoun, S., Papadopoulos, M.C., Watanabe, H., Yan, D., Manley, G.T., and Verkman, A.S. (2005). Involvement of aquaporin-4 in astroglial cell migration and glial scar formation. J. Cell Sci. 118, 5691–5698.
16. Abbott, N.J., Ronnback, L., and Hansson, E. (2006). Astrocyte-endothelial interactions at the blood-brain barrier. Nat. Rev. Neurosci. 7, 41–53.
17. Bush, T.G., Puvanachandra, N., Horner, C.H., Polito, A., Ostenfeld, T., Svendsen, C.N., Mucke, L., Johnson, M.H., and Sofroniew, M.V. (1999). Leukocyte infiltration, neuronal degeneration, and neurite outgrowth after ablation of scar-forming, reactive astrocytes in adult transgenic mice. Neuron 23, 297–308.
18. Myer, D.J., Gurkoff, G.G., Lee, S.M., Hovda, D.A., and Sofroniew, M.V. (2006). Essential protective roles of reactive astrocytes in traumatic brain injury. Brain 129, 2761–2772.
19. Wetherington, J., Serrano, G., and Dingledine, R. (2008). Astrocytes in the epileptic brain. Neuron 58, 168–178.
20. Del Vecchio, R.A., Gold, L.H., Novick, S.J., Wong, G., and Hyde, L.A. (2004). Increased seizure threshold and severity in young transgenic CRND8 mice. Neurosci. Lett. 367, 164–167.
21. Ma, T., Yang, B., Gillespie, A., Carlson, E.J., Epstein, C.J., and Verkman, A.S. (1997). Generation and phenotype of a transgenic knockout mouse lacking the mercurial-insensitive water channel aquaporin-4. J. Clin. Invest. 100, 957–962.
22. Roberson, E.D., Scearce-Levie, K., Palop, J.J., Yan, F., Cheng, I.H., Wu, T., Gerstein, H., Yu, G., and Mucke, L. (2007). Reducing endogenous tau ameliorates amyloid β-induced deficits in an Alzheimer's disease mouse model. Science 316, 750–754.
23. Sanchez Mejia, R.O., Ona, V.O., Li, M., and Friedlander, R.M. (2001). Minocycline reduces traumatic brain injury-mediated caspase-1 activation, tissue damage, and neurological dysfunction. Neurosurgery 48, 1393–1399; discussion, 1399–1401.
24. Yrjanheikki, J., Tikka, T., Keinanen, R., Goldsteins, G., Chan, P.H., and Koistinaho, J. (1999). A tetracycline derivative, minocycline, reduces inflammation and protects against focal cerebral ischemia with a wide therapeutic window. Proc. Natl. Acad. Sci. U. S. A. 96, 13496–13500.
25. Papadopoulos, M.C., Saadoun, S., and Verkman, A.S. (2008). Aquaporins and cell migration. Pflugers Arch. 456, 693–700.
26. Dowding, A.J., and Scholes, J. (1993). Lymphocytes and macrophages outnumber oligodendroglia in normal fish spinal cord. Proc. Natl. Acad. Sci. U. S. A. 90, 10183–10187.
27. Perry, V.H., and Andersson, P.B. (1992). The inflammatory response in the CNS. Neuropathol. Appl. Neurobiol. 18, 454–459.
28. Carson, M.J., and Sutcliffe, J.G. (1999). Balancing function vs. self defense: the CNS as an active regulator of immune responses. J. Neurosci. Res. 55, 1–8.
29. Hirschberg, D.L., and Schwartz, M. (1995). Macrophage recruitment to acutely injured central nervous system is inhibited by a resident factor: a basis for an immune-brain barrier. J. Neuroimmunol. 61, 89–96.
30. Riazi, K., Galic, M.A., Kuzmiski, J.B., Ho, W., Sharkey, K.A., and Pittman, Q.J. (2008). Microglial activation and TNFα production mediate altered CNS excitability following peripheral inflammation. Proc. Natl. Acad. Sci. U. S. A. 105, 17151–17156.
31. Chu, L.S., Fang, S.H., Zhou, Y., Yin, Y.J., Chen, W.Y., Li, J.H., Sun, J., Wang, M.L., Zhang, W.P., and Wei, E.Q. (2010). Minocycline inhibits 5-lipoxygenase expression and accelerates functional recovery in chronic phase of focal cerebral ischemia in rats. Life Sci. 86, 170–177.
32. Tang, M., Alexander, H., Clark, R.S., Kochanek, P.M., Kagan, V.E., and Bayir, H. (2010). Minocycline reduces neuronal death and attenuates microglial response after pediatric asphyxial cardiac arrest. J. Cereb. Blood Flow Metab. 30, 119–129.
33. Wu, J., Yang, S., Hua, Y., Liu, W., Keep, R.F., and Xi, G. (2010). Minocycline attenuates brain edema, brain atrophy and neurological deficits after intracerebral hemorrhage. Acta Neurochir. Suppl. 106, 147–150.
34. Yang, F., Liu, Z.R., Chen, J., Zhang, S.J., Quan, Q.Y., Huang, Y.G., and Jiang, W. (2010). Roles of astrocytes and microglia in seizure-induced aberrant neurogenesis in the hippocampus of adult rats. J. Neurosci. Res. 88, 519–529.
35. Bordey, A., Hablitz, J.J., and Sontheimer, H. (2000). Reactive astrocytes show enhanced inwardly rectifying K^+ currents in situ. Neuroreport 11, 3151–3155.
36. Connors, N.C., Adams, M.E., Froehner, S.C., and Kofuji, P. (2004). The potassium channel Kir4.1 associates with the dystrophin-glycoprotein complex via alpha-syntrophin in glia. J. Biol. Chem. 279, 28387–28392.
37. Tait, M.J., Saadoun, S., Bell, B.A., and Papadopoulos, M.C. (2008). Water movements in the brain: role of aquaporins. Trends Neurosci. 31, 37–43.
38. Traynelis, S.F., and Dingledine, R. (1989). Role of extracellular space in hyperosmotic suppression of potassium-induced electrographic seizures. J. Neurophysiol. 61, 927–938.
39. Verkman, A.S., Binder, D.K., Bloch, O., Auguste, K., and Papadopoulos, M.C. (2006). Three distinct roles of aquaporin-4 in brain function revealed by knockout mice. Biochim. Biophys. Acta 1758, 1085–1093.

Address correspondence to:
Geoffrey T. Manley, MD, PhD
Department of Neurosurgery
University of California, San Francisco
1001 Potrero Avenue
Building 1, Room 101
San Francisco, CA 94110
USA

E-mail: Manleyg@neurosurg.ucsf.edu